Electronic Supplementary Material (ESI) for Journal of Materials Chemistry B.

Near-infrared light photoelectrochemical immunosensor based on Au-paper electrode and naphthalocyanine sensitized ZnO nanorods

Guoqiang Sun [a], Panpan Wang [a], Peihua Zhu [a], Lei Ge [a], Shenguang Ge [b], Mei Yan [a], Xianrang Song [c] and Jinghua Yu *[a]

[a] *Key Laboratory of Chemical Sensing & Analysis in Universities of Shandong, University of Jinan, Jinan 250022, China.*

[b] *Shandong Provincial Key Laboratory of Preparation and Measurement of Building Materials, University of Jinan, Jinan 250022, China.*

[c] *Cancer Research Center, Shandong Tumor Hospital, Jinan 250012, P.R. China.*

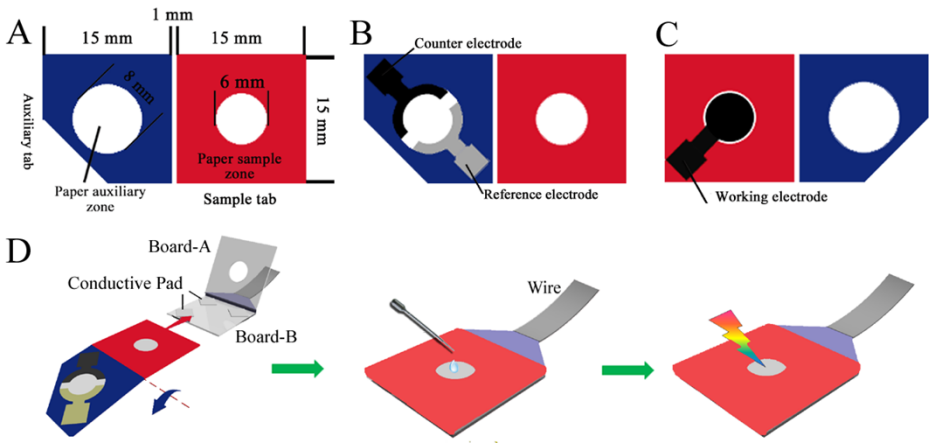

Scheme S1. (A) The schematic representation, size and shape of this disposable microfluidic PEC origami device; (B) One side of the μ-PECOD with the screen-printed reference and counter electrode; (C) The reverse side of (B) with the screen-printed working electrode; (D) Schematic representation of the assay procedures for this μ-PECOD.

Preparation of the μ-PECOD

The preparation of this μ-PECOD was similar to our previous work[1] with modifications and a detailed procedure was described below. Wax was used as the paper hydrophobization and insulation agent in this work to construct the hydrophobicbarrier on the paper. As shown in Scheme S1A, this origami device was comprised of a square auxiliary tab (15.0 mm × 15.0 mm) and a square sample tab (15.0 mm × 15.0 mm). An angle of the square auxiliary tab was cut off for exposure of the contact pad of the screen-printed carbon working electrode. The shape of the hydrophobic barrier on the origami device, which contains a paper auxiliary zone (8 mm in diameter) on the auxiliary tab, and a paper sample zone (6.0 mm in diameter) on the sample tab, respectively, was designed using Adobe illustrator CS4. The entire origami device could be produced in bulk on an A4 paper sheet using a commercially available solid-wax printer (Xerox Phaser 8560N color printer). Owing to the porous structure of paper, the melted wax can penetrate into the paper network to decrease the hydrophilicity of paper remarkably. After the curing process, the unprinted area (paper auxiliary zone and paper sample zone) still maintained good hydrophilicity, flexibility, and porous structure and will not affect the further screen-printing of electrodes and modifications.

Between the sample tab and auxiliary tab, the unprinted line (1 mm in width) was defined as the fold line, which could ensure that the paper sample zone on the sample tab was properly and

exactly aligned to the auxiliary zone on the auxiliary tab after folding (Scheme S1A), due to the difference of flexibility between the printed and unprinted area after baking. The unprinted hydrophilic area (paper auxiliary zone and paper sample zone) constituted the reservoir of the paper PEC cell (~40 μL) after being folded at the predefined fold line. Then, the wax-penetrated paper sheet was ready for screen-printing of the electrode containing the wire and contact pad on its corresponding paper zone (Scheme S1B and S1C). Due to the small size of the origami device, the silver wire and contact pad in a traditional screen-printed electrode can be directly replaced by carbon ink and Ag/AgCl ink respectively. The electrode array consisted of a screen-printed Ag/AgCl reference electrode and a carbon counter electrode on the auxiliary zone (Scheme S1B) and a screen-printed carbon working electrode (6 mm in diameter) on the reverse side of the paper sample zone (Scheme S1C), respectively. After folding, the three screen-printed electrodes (working electrode, reference electrode, and counter electrode) will be connected once the paper PEC cell has been filled with solution. Finally, the paper sheet was cut into individual origami devices for further modifications.

Optimization of the experimental conditions

To optimize the experimental condition for CEA measurement, the effects of incubation temperature and time for the antibody-antigen interaction, applied potential and the concentration of AA were investigated. Considering the immunoreaction, the region of 20-55 °C was chosen to investigate the effect of reaction temperature (Fig. S1A). The photocurrent responses decrease with increasing temperature up to 37 °C, which was attributed to the increasing immunoreaction rate between anti-CEA antibodies and CEA. The higher temperature caused an irreversible denaturation of proteins, thus, photocurrent responses increase. In the following experiments, 37 °C was employed as the optimal incubation temperature for further studies.

The influence of the immunoreactions time on response signals was also investigated (Fig. S1B). With the increase of incubation time at 37 °C, the photocurrent intensity decreased. When the interaction time was over 300 s, the photocurrent response of the immunosensor was constant, indicating that the interaction reached equilibrium. Thus, 300 s was chosen as the immunoreaction time.

Applied potential was an important factor relevant to the photocurrent response. As shown in Fig. S1C, with an increase of potential from -0.4 to 0 V, the photocurrent increases sharply. A negative potential can inhibit the electron driven to the electrode, which may lead to the electron hole recombination. In the potential range from 0 to 0.2 V, the photocurrent also sharply improved. However, the photocurrent at 0 V showed acceptable sensitivity for the PEC detection of CEA. The low applied potential was beneficial to the elimination of interference from other reductive species that coexisted in the real samples. Therefore, 0 V was selected as the applied potential for the determination of CEA.

In the experiments, changing the concentration of AA, different photocurrent was obtained (Fig. S1D). As a hole scavenger, when the concentration of AA was lower than 0.1 mol L^{-1}, the photocurrent increased with increasing AA concentration; when the concentration of AA was further elevated, the photocurrent would decrease with increasing concentration of AA. This may be attributed to a much higher concentration of AA would result in the increase of the absorbance of AA in solution, as a consequence, the intensity of the irradiation arriving at the electrode surface decreased and the efficiency of excited ZnNc-COOH would decrease. Therefore, 0.1 mol L^{-1} AA was chosen for the following experiments.

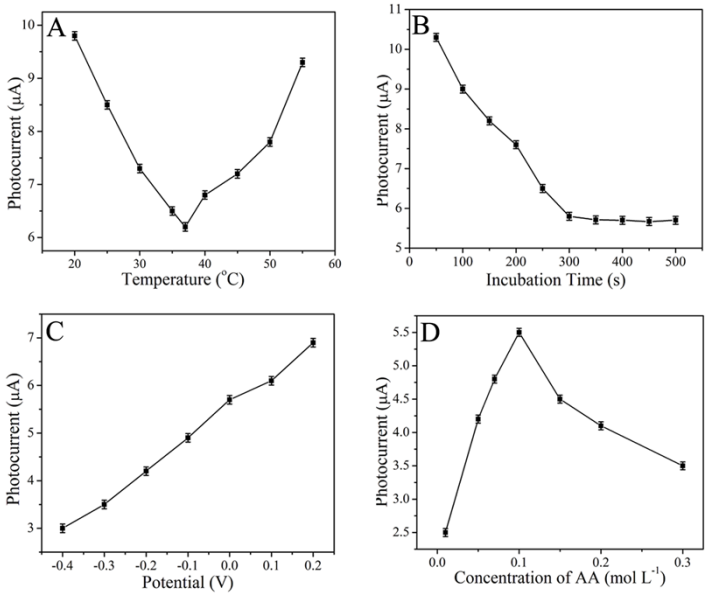

Fig. S1. Effect of (A) incubation temperature, (B) incubation time, (C) applied potential and (D) concentration of AA on photocurrent responses of Ab_1/ZnNc-COOH/ZnO NRs/Au-PWE after incubated in CEA solution (1.0 ng mL^{-1}).

Table S1. Comparison of analytical properties of different immunoassays toward CEA

Measurement protocol	Linear ($ng\ mL^{-1}$)	Detection limit ($pg\ mL^{-1}$)	References
Electrochemical immunoassay	2.0-20	1000	2
Chemiluminescent immunoassay	0-50	5.0	3
Surface plasmon resonance immunoassay	3-400	3000	4
Flow injection electrochemical	0.5-25	220	5
PEC immunoassay	0.05-20	10	6
μ-PECOD	0.005-100	1.6	This work

References

1 J. J. Lu, S. G. Ge, L. Ge, M. Yan and J. H. Yu, *Electrochim. Acta*, 2012, **80**, 334-341.

2 J. H. Lin, W. Qu and S. S. Zhang, *Anal. Sci.*, 2007, **27**, 1059-1063.

3 S. X. Qu, J. T. Liu, J. P. Luo, Y. Q. Huang, W. T. Shi, B. Wang and X. X. Cai, *Anal. Chim. Acta*, 2013. **766**, 94-99.

4 Z. Altintas, Y. Uludag, Y. Gurbuz and I. E. Tothill, *Talanta*, 2011, **86**, 377-383.

5 J. Wu, T. H. Tang, Z. Dai, F. Yan, H. X. Ju and N. E. Murr, *Biosens. Bioelectron.*, 2006, **22**, 102-108.

6 W. W. Tu, W. J. Wang, J. P. Li, S. Y. Deng and H. X. Ju, *Chem. Commun.*, 2012, **48**, 6535-6537.